HOSTED BY

ELSEVIER

Contents lists available at ScienceDirect

Engineering Science and Technology, an International Journal

journal homepage: www.elsevier.com/locate/jestch

JESTECH

CrossMark

Full Length Article

Manufacturing of new roughness standards for the linearity of the vertical axis – Feasibility study and optimization

Matthias Eifler [a,*], Frank Schneider [b], Jörg Seewig [a], Benjamin Kirsch [b], Jan C. Aurich [b]

[a] Institute for Measurement and Sensor-Technology, Department of Mechanical and Process Engineering, University of Kaiserslautern, Gottlieb-Daimler-Straße, Kaiserslautern D-67663, Germany
[b] Institute for Manufacturing Technology and Production Systems, Department of Mechanical and Process Engineering, University of Kaiserslautern, Gottlieb-Daimler-Straße, Kaiserslautern D-67663, Germany

ARTICLE INFO

ABSTRACT

In order to provide an alternative for the vertical axis calibration of stylus instruments which is usually performed based on step height standards, a new measurement standard geometry for the calibration of the linearity and research on its manufacturing is needed. For the manufacturing of these geometric measurement standards there is, according to the type of the measurement standard, a broad range of manufacturing processes that can be applied. New measurement standards for the roughness calibration were developed at the University of Kaiserslautern and an ultra-precision turning process was chosen for its manufacturing. The paper presents a feasibility study of the chosen manufacturing process. The aim of the investigations is to present the development of the standard and the qualification of the ultra-precision turning process for the manufacturing of calibration standards. An examination was performed in order to characterize the influences of different process parameters on the quality of the manufactured roughness standard.

1. Introduction

In today's industry, topography measuring instruments that measure given profiles with a high accuracy are required. Therefore, a proper calibration of the devices with different measurement standards is essential. As a roughness standard, statistically distributed as well as defined microstructures are suitable for calibration purposes. A trend in precision engineering however is the application of more deterministic surfaces, e.g. riblet structures [1]. For roughness calibration, generally artificial structures with a statistically distributed surface are used that are non-problematic for measurement devices. To manufacture measurement standards different manufacturing processes can be applied. In addition to chemical processes as for example the wet etching process used by Frühauf et al. to manufacture triangular gratings for a surface texture standard [2] mechanical processes like cutting and abrasive processes are convenient. Frühauf et al. used lapping [3] to manufacture areal roughness standards. The resulting roughness parameters of the standard are mainly depending on the size of

the used grains. To manufacture nano-roughness standards used for the calibration of atomic force microscopes, Gatzen et al. applied a nano-grinding process [4]. The results prove the applicability of the nano-grinding with an average roughness of 21 nm.

In order to perform a calibration that is closer to the application, the use of deterministic measurement standards that are based on engineering surfaces is reasonable because statistical surfaces generally do not represent the characteristics of a real measurement task. For the manufacturing of deterministic measurement standards, ultra-precision manufacturing methods are necessary as the requirements for the precision of calibrating and measuring processes are constantly increasing. This is valid for surfaces in general, but even more for the surfaces of geometric measurement standards. As a consequence, manufacturing processes that can meet the requirements to generate defined microstructures are increasingly needed for the manufacturing of roughness standards. Ultra-precision cutting processes are suitable to manufacture defined structures due to the large number of machinable materials and the great diversity of possible geometries [5]. Nemoto developed and manufactured an areal standard using a diamond ball end mill [6]. It was ascertained that turning is a suitable method for the generation of measurement standards with a defined profile [7].

Due to the high costs of the manufacturing processes to produce roughness standards, mainly the so called master standard is

* Corresponding author.
E-mail address: meifler@mv.uni-kl.de (M. Eifler).
Peer review under responsibility of Karabuk University.

produced and duplicated in a replication process. There are different methods for the replication of micro and nano surface geometries [8]. The development of a cost efficient electroforming process was investigated by Leach [9].

In the ISO 25178-600 (see e.g. [10,11]) series, the topic of height axis calibration is addressed. ISO 25178-600 is currently under preparation and introduces the so called "metrological characteristics". For the height axis not only the linearity deviation is named, but as well the determination of the amplification coefficient, the topography fidelity as e.g. proposed in [12], flatness, noise and the topographic spatial resolution (see e.g. [10,11]). Specific guidelines are available for different measurement principles: e.g. for stylus instruments there are definitions in ISO 25178-601 [10], for phase-shifting interferometers in ISO 25178-603 [11]. According calibration strategies for optical topography measurement devices which consider the metrological characteristics were introduced [13–15] as well as an according set of measurement standards [16]. As a chosen example, a new linearity standard for the vertical axis (z-axis) is examined in the research presented in this paper. The calibration of the z-axis is usually performed with step height standards [14]. One aim of the z-calibration is the detection of linearity errors [14].

Considering the metrological characteristics [10,11], the linearity deviation and the amplification coefficients are the relevant instrument properties to examine. For the detection of linearity errors there are a few measurement standards in the international standardization which can be used for the calibration of the vertical axis. These include the 2D step height standard, type A of ISO 5436-1 [17], as well as different 3D step height standards defined in ISO 25178-70 [18].

All these standards have in common that only discrete step values are used representatively to calibrate the entire axis. Thus only a small fraction of the measuring range is addressed as discrete measuring values because only pre-fabricated structures are used. Another issue is that the measurement result of a step height differs for example within the piezo range [19]. To achieve more precise measurement results, there is the need of calibrating the entire measurement range [19]. Usually it is not satisfactory to use one step height standard for the calibration, instead many different step height values are required [20].

To improve calibration quality, a multi-step height standard was developed within the project "KalWint" at the PTB (Physikalisch-Technische Bundesanstalt), shown in [21]. This measurement standard has the characteristic of multiple steps in the

micro- as well as the macro-model and thus allows a wider calibration of the measurement range than measurement standards with just one or a few steps [22].

A further improvement would be the calibration with continuous height values instead of discrete values. A suitable approach is introduced in the following in order to overcome the given limitations by the use of step height standards. Therefore, a measurement standard is generated by a model-based approach that images a certain characteristic of the Abbott-curve and therefore allows an almost continuous calibration of the height axis which is only limited by the spatial resolution of the executed sampling. The Abbott-curve represents the height distribution of a given profile and is thus a suitable tool for the height axis calibration. Within this paper, an investigation of the general feasibility of an ultra-precision turning process for the purpose of manufacturing such new developed deterministic roughness standards is performed.

2. The design approach of the examined linearity standard

At the University of Kaiserslautern, a new approach for the design of measurement standards was developed [23]. The general idea is to modify real, measured surfaces in a way that they can be used as a measurement standard [23]. This means that the calibration can be performed in a very practical manner and that no artificial structures are used [23]. This approach is an improvement to the current strategies that usually use artificial roughness structures that are not related to the later performed measurement task.

The design of the roughness standards is determined with a model-based approach which is illustrated in Fig. 1. The Abbott-curve of a profile is determined and transformed in a way that the desired characteristics for the calibration are met. Through the manufacturing, measuring, filtering and parameter calculation process different physical effects occur. For example, the geometry of the tool and the stylus tip have an effect on the examined profile and its roughness parameters.

Therefore, an entire virtual process chain is imaged in order to consider these effects. This includes a virtual modelling of the manufacturing process that calculates the influence of the tool's geometry on the surface, the measuring process, which considers the morphological filtering of the stylus tip and the evaluation. The modelling of the manufacturing process is discussed in depth in Section 3.1. After the application of the virtual signal chain, a new profile is obtained that is checked regarding a given
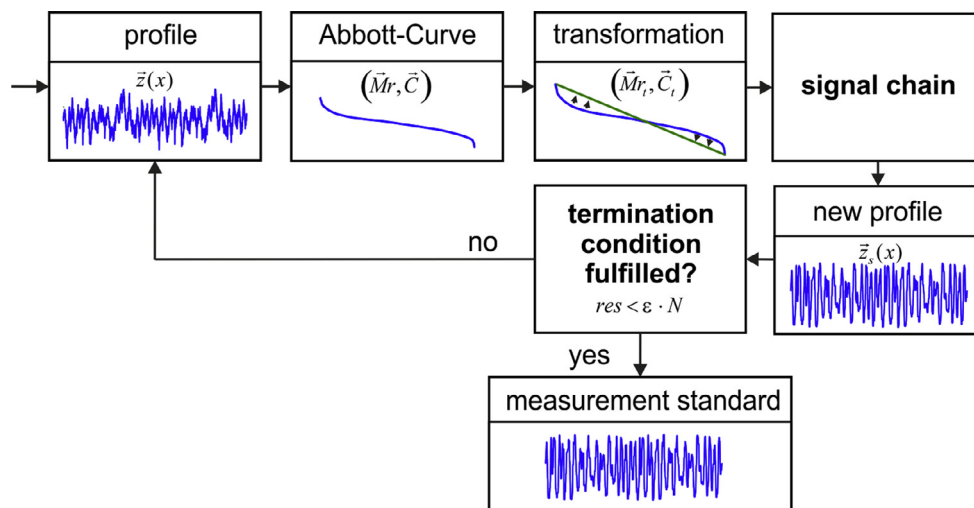

Fig. 1. Design approach for the measurement standard.

termination condition. An iterative approach is chosen: when the termination condition is fulfilled, the control dataset for the manufacturing of the desired roughness standard is the result. Otherwise, the transformation is executed again.

The geometry of the examined measurement standard is based on the imaging of a linear Abbott-curve [23]. The measurement data of a rough surface is transformed towards this linear Abbott-curve. The corresponding transformation is introduced in the following.

The Abbott-curve is mathematically defined by plotting the height $\vec{C}$ of a profile as a function of the associated material ratio $\vec{Mr}$. For discrete values of a profile $\vec{z}(x)$ with N values the Abbott-curve is defined as $\left(\vec{Mr}, \vec{C}\right)$ where:

$$\vec{Mr} = \begin{pmatrix} Mr_1 \\ \vdots \\ Mr_N \end{pmatrix}, \ \vec{C} = \begin{pmatrix} C_1 \\ \vdots \\ C_N \end{pmatrix} \tag{1}$$
$$(Mr_k, C_k) = \left(\tfrac{k-1}{N-1}, C_k\right), \ k = 1, 2, \ldots, N$$

with the sorted, discrete profile values, where C_k represents the k-th largest value of $\vec{z}(x)$.

The target Abbott-curve is defined from the highest peak to the deepest valley and covers a material ratio of 0–100%. The two points $(0; C_{1,act})$ and $(100; C_{N,act})$ are connected with a straight line. A straight line of the scheme

$$\vec{C}_{tar} = \begin{pmatrix} C_{1,tar} \\ \vdots \\ C_{N,tar} \end{pmatrix}, \ C_{k,tar} = a \cdot \frac{k-1}{N-1} + b; k = 1, 2, \ldots, N \tag{2}$$

with the slope a and the z-axis intercept b is applied. The two parameters can be determined based on the actual Abbott-curve:

$$a = \frac{\Delta C_{act}}{\Delta\left(\frac{k-1}{N-1}\right)} = C_{N,act} - C_{1,act}; \ \text{for } k = N; \ b = C_{1,act}. \tag{3}$$

The transformation instruction Ψ for the j-th z-value $z(x_j)$ is executed:

$$z_t(x_j) = \Psi(z(x_j)), \ j = 1, 2, \ldots, N. \tag{4}$$

The transformed height value $z_t(x_j)$ in order to achieve the desired Abbott-curve is:

$$z_t(x_j) = -\frac{\sum_{i=1}^{N} n_i}{N} \cdot a + b; \quad n_i = \begin{cases} 1 \text{ for } z(x_i) > z(x_j) \\ 0 \text{ for } z(x_i) \leqslant z(x_j) \end{cases}. \tag{5}$$

The summation of n_i determines the height index of the profile point, corresponding to the number of profile points that have a bigger height value than $z(x_j)$. This index is used to calculate the ratio to the total number of profile points. In the actual transformation this ratio is multiplied with the amplitude of the profile, leading to a straight line Abbott-curve. The results are the transformed values

$$\vec{z}_t = (z_t(x_j)), \ j = 1, 2, \ldots, N. \tag{6}$$

As shown in Fig. 1, the strength of the new approach is the consideration of the physical effects that occur during manufacturing and sampling (referred to as "signal chain"). The transformed profile has to undergo the described virtual signal chain in order to consider these effects after the transformation which leads to the profile $\vec{z}_s(x)$.

Because both criteria of the linear Abbott-curve as well as the manufacturing feasibility have to be ensured, iteration is necessary. As illustrated, after the virtual process chain the new profile is checked regarding the given termination condition, and, if neces-

sary, put under the transformation again. For the examination of the termination condition for every separate point of the Abbott-curve the deviation between actual and target Abbott-curve is determined and this deviation is summed up. A residuum ε can be provided, which is the maximum average difference for every single profile point. This leads to a total residuum of

$$res = \sum_{j=1}^{N} |C_{j,act} - C_{j,tar}| < \varepsilon \cdot N \tag{7}$$

for N data points. If this criterion is fulfilled the transformation is complete.

The transformation can be applied to an arbitrary profile. This is the strength of the approach which preserves the height ranking order of the original profile throughout the transformation. As an example for an application the surface of a commercial Halle Roughness Standard was undergone the transformation. Fig. 2 shows the original profile as well as the associated Abbott-curve and the transformed profile with the Abbott-curve after the filtering. The target roughness parameters of the resulting profile after the application of the virtual signal chain are: $R_{a,tar} = 1.5765$ µm, $R_{q,tar} = 1.8203$ µm and $R_{z,tar} = 6.1041$ µm.

The resulting surface can be properly used for a calibration because the z-values are continuously spread to every height level. This means that an almost stepless calibration of the z-axis can be executed. The result is that the limitations of step height standards [17,18], where usually just one or a few height values are calibrated [14,20] can be overcome. When using step height standards, only their discrete height values are calibrated. Possible linearity deviations in between those discrete steps cannot be detected. This means: the more height values are used, the more accurate is the executed calibration. Following this principle, the introduced standard allows a number of steps equivalent to the number of sampling points. As the Abbott-Curve represents the distribution of height values within a profile, a linearity calibration can be executed based on this criterion. This results in a calibration approach which is able to calibrate the entire height measurement range throughout the entire lateral measurement range within only one measurement.

The resulting Abbott-curve can thus be calibrated to consider possible deviations within the process chain. For the later performed manufacturing, the profile with a length of 4 mm is manufactured four times consecutively. Due to this performed periodical continuation the measurement results do not depend on the measuring position. As a cutoff-wavelength of $\lambda_c = 0.8$ mm should be used, this characteristic is similar to conventional roughness standards (see e.g. [24]). The entire profile is imaged in every arbitrary standard 4 mm evaluation area. To perform the evaluation of the measurement results a least-squares fit of the measured Abbott-curve is applied. The deviation to the nominal Abbott-curve is plotted versus the height of the profile and certain non-linearities of the z-axis can be located and quantified quickly. The evaluation and calibration strategy for the designed standard is discussed in depth later. Based on these requirements, a control dataset for the machine tool was calculated on the basis of iteration. This control dataset is the result of the iteration shown in Fig. 1 and defines the geometry of the standard to be manufactured.

3. Experimental setup

3.1. Dimensioning the geometry due to considerations of the manufacturing process

For the manufacturing of the introduced roughness standard, an ultra-precision turning process using a monocrystalline diamond tool was chosen. For the dimensioning of the geometric features
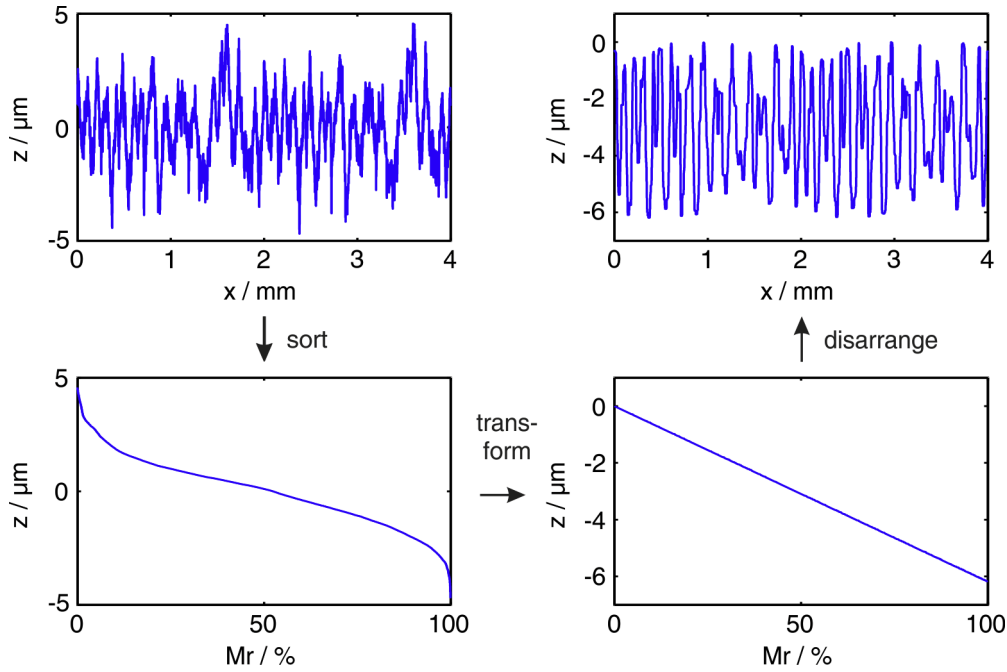
Fig. 2. Linearity standard, profile before and after the transformation and associated Abbott-curves.

of the measurement standard and the desired control dataset the geometry of the tool has to be known. In other investigations it has been shown that the measurement of the micro shape of tools is possible with different measuring principles, see e.g. [21]. The measurement process of the tool is as well uncertain. One possibility for the estimation of the measurement uncertainty of lateral structure sizes is the determination based on the finite size of a pixel. The approach in Fig. 3 is chosen for a more exact consideration of the manufacturing effects: the tool's geometry is measured with a confocal microscope. An objective that provides measurement data with a lateral discretization distance of 0.625 μm is used. When performing a distance measurement of two points, the total discretization uncertainty is added up to approximately the value of the pixel size with uniform distribution. Therefore the chamfer width b can be characterized to:

$$b = (10.0 \pm 0.625) \text{ μm}. \tag{8}$$

The second parameter of the tool's geometry is its corner angle ε which is determined as:
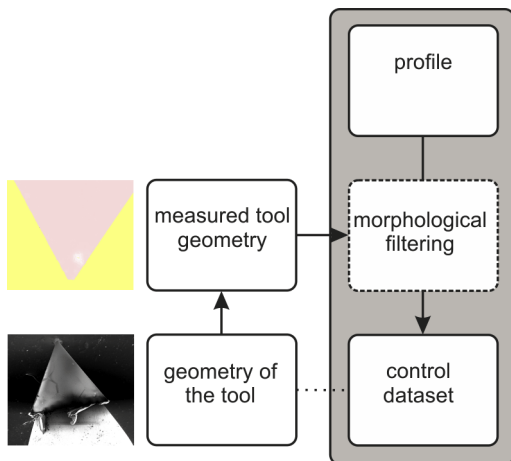

Fig. 3. Consideration of effects resulting from the tool geometry.

$$\varepsilon = (57.7 \pm 1.7)^\circ. \tag{9}$$

With the obtained measurement data, the actual geometry of the tool can be modelled and considered within the virtual manufacturing process of the signal chain (as given in Fig. 1).

The measured geometry of the tool is implemented in the profile with the aid of a morphological filter according to ISO 16610-41 [25,26]. The "virtual manufacturing process" step is integrated into the algorithm for the calculation of the dataset. The tool's shape is the structuring element of the filter. A detailed description of the manufacturing process is given in chapter 3.2. The manufactured roughness standard is measured to examine the compliance with the target data. An overview of the interdependencies between the tool's geometry and the modelling of the manufacturing process is given in Fig. 3.

3.2. Manufacturing process

The roughness standards were manufactured using a diamond machining process (Fig. 4). Therefore the ultra-precision lathe MTC 250 (LT-Ultra) with a high stiffness and movement in the nanoscale was used to achieve the necessary small interpolation steps of the CNC Code based on the virtual dataset. The workpiece was clamped on the air bearing spindle.

In a preceding face turning process the workpiece was processed to achieve the necessary flat surface. Therefore a monocrystalline diamond (MCD) tool brazed on a cemented carbide substrate (Tool 1) with a large corner radius r_ε was used to achieve a small kinematic roughness. For the manufacturing of the microstructures of the standard a MCD-tool (Tool 2) with a special tip geometry was used. The nominal tool geometries of the two tools are listed in Table 1. The determination of the actual geometry of tool 2 was described in Section 3.1. This actual geometry was considered within the design process of the measurement standard.

3.3. Measurement and evaluation process

A tactile measurement device (Hommel T 8000) was used for the examination. A stylus tip with a radius of 5 μm and an angle
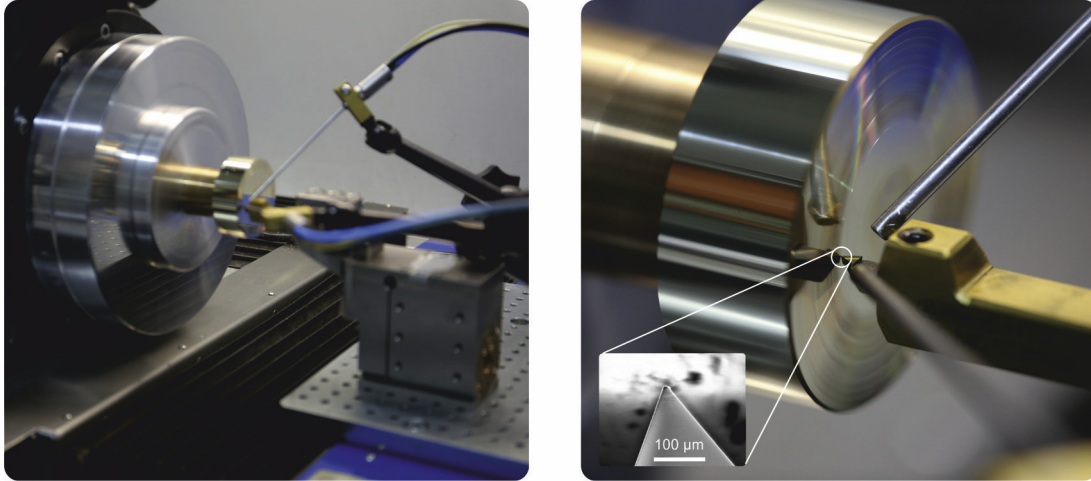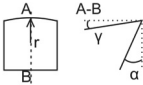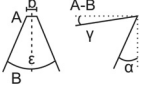
Fig. 4. Experimental setup.

Table 1
Tool geometry, nominal values.

Tool geometry		
Tool 1		
Rake angle γ	0°	
Clearance angle α	10°	
Corner radius r	50 mm	
Tool 2		
Rake angle γ	0°	
Clearance angle α	10°	
Corner angle ε	55°	
Chamfer width b	10 µm	

of 90° was used. Further, a traverse speed of 0.5 mm/s was applied. As the measurement standard was specifically designed for the applied tip geometry, also possible changes of the tip shape might be detectable with the calibration procedure. The sampling process was considered within the design of the standard (see Section 2), and so an application of the approach for arbitrary measurement procedures is possible as long as the physical effects of the sampling are considered within the design of the measurement standard [23].

The manufactured measurement standard and the measurement and evaluation positions are shown in Fig. 5. The measurement of each manufactured standard was performed at 36 measuring positions (every 10°) in order to perform samplings throughout the entire measurement standard. The evaluation positions start every 200 µm. This means that each measuring position consists of 53 evaluation positions when a standard evaluation length of 4 mm and the filter running-in and running-out-lengths are considered. The linear Gaussian filter [27] was used with $\lambda_c = 0.8$ mm. In sum this means that there are 1908 measurement values for each standard. An evaluation of the roughness profile parameters R_a, R_q and R_z was performed. These roughness parameters indicate a possible deviation of the Abbott-curve.

An important criterion for the standard is its linearity. The linearity deviation can be characterized with different criteria. Two different evaluations are used: first, a new parameter is introduced that can serve for a characterization of the linearity. Further, it can be shown that also with the new measurement standards an application of the present ISO 25178-600 series is possible.

For the new evaluation routine, a Least Squares straight line fit is performed with the data of the measured Abbott-curve meaning the relevant z-intercept and the slope of the straight line are calcu-

lated. The difference between the fitted line and the measurement data is calculated pointwise and averaged to achieve the linearity deviation value ld. With the measured profile:

$$\overrightarrow{z}_{ms} = \begin{pmatrix} z_{ms,1} \\ \ldots \\ z_{ms,N} \end{pmatrix}, \tag{10}$$

the measured Abbott-curve is determined, where $C_{ms,k}$ represents the k-th largest value of $\overrightarrow{z}_{ms}$:

$$\overrightarrow{C}_{ms} = (C_{ms,k}), \ k = 1, 2, \ldots, N, \tag{11}$$

$$\overrightarrow{M}r_{ms} = (Mr_{ms,k}), \ Mr_{ms,k} = \frac{k-1}{N-1}, \ k = 1, 2, \ldots, N. \tag{12}$$

The fit of the Abbott-curve is modelled as:

$$\overrightarrow{C}_{fit_1} = (C_{fit_1,k}), \ C_{fit_1,k} = a_{ms} \cdot Mr_{ms,k} + b_{ms_1}, \ k = 1, 2, \ldots, N, \tag{13}$$

indicating a straight line fit with the slope a_{ms} and the intercept bms_1. This fit leads to the linearity deviation ld:

$$ld = \frac{\sum_{k=1}^{N} |C_{ms,k} - C_{fit_1,k}|}{N}. \tag{14}$$

As the measurement standard is designed for a calibration of the z-axis linearity, further an evaluation according to the ISO 25178-600 series can be excuted. In doing so, the measured height values are plotted as a function of the target height values of the measurement standard to define the transfer function $(C_{k,tar}, C_{ms,k})$, $k = 1, 2, \ldots, N$ of the z-axis. A Least-Squares Fit $\overrightarrow{C}_{fit_2}$ of this transfer function is executed. As the most significant linearity deviations are expected at the margins of the measurement range, another fit $\overrightarrow{C}_{fit_3}$ is executed with the inner 80% of the measured values:

$$\overrightarrow{C}_{fit_{2,3}} = \left(C_{fit_{2,3},k}\right), \ C_{fit_{2,3},k} = \alpha_{z_{2,3}} \cdot C_{tar,k} + b_{ms_{2,3}}, \ k = 1, 2, \ldots, N. \tag{15}$$

Here, the slopes of the fitted straight lines are the amplification coefficients $\alpha_{z_{2,3}}$ as defined in ISO 25178-600 and the according linearity deviations are the maximum deviation between the fitted line and the transfer function:

$$ld_{ISO_{2,3}} = \max_{k=1,2,\ldots,N} (C_{fit_{2,3},k} - C_{ms,k}). \tag{16}$$
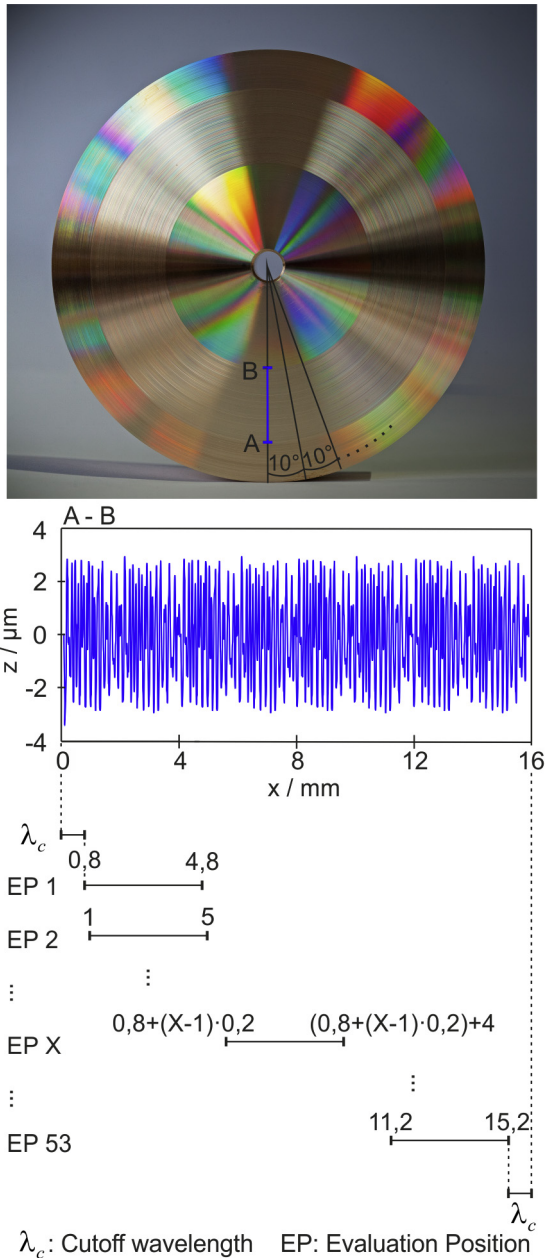
Fig. 5. Manufactured measurement standard and its measurement and evaluation positions.

It was stated that the metrological characteristics are defined for stylus instruments as well as optical instruments. The proposed standard is suitable for calibrating the amplification coefficient and the linearity deviation. However regarding optical instruments there is the limitation that their topography fidelity is influenced by the local slope [28,29]. For the characterization of the profile fidelity there are however other suitable measurement standards, e.g. the chirp standard [26,12]. The results of the different measurements analyzing the amplification coefficient and the linearity deviations are given in the following section.

A calibration of e.g. a stylus instrument with the proposed measurement standard can be executed with very little effort as only one measurement of the given structure is required in order to characterize the described roughness parameters and linearity parameters.

4. Feasibility analysis and a generic parameter study

The general feasibility was demonstrated by the manufacturing of a reference standard. The results of the measurement with the stylus instrument are shown in Table 2. When the roughness parameters are examined according to the described measuring and evaluating strategy, the average values differ within the range of a few percent and have a standard deviation within the nanometer range. When the measured and the target profile are compared, there is a good accordance as shown in Fig. 6. Both the target profile and the target Abbott-curve are imaged precisely.

In order to examine further possible applications of the designed standard, an examination regarding the suitability for the use with optical measurement devices was performed. For this purpose, a confocal microscope was used with a 20× objective (Numerical Aperture of 0.6). Four topographies were extracted along the entire structure every 90°. Six profiles of every topography (24 in total) were evaluated with 53 evaluations each extracted from the dataset every 200 μm. This leads to a total number of 1272 evaluation spots. The resulting values of the measurement of the reference standard are listed in Table 2.

The results indicate that the standard is as well suitable for the use with optical measurement devices. However, due to the different physical measurement principle, the results of optical and stylus instruments differ. One reason for that was given in the previous section: when using optical measurement the local slope of the surface and flatness deviations influences the measurement

Table 2
Results of the reference standard.

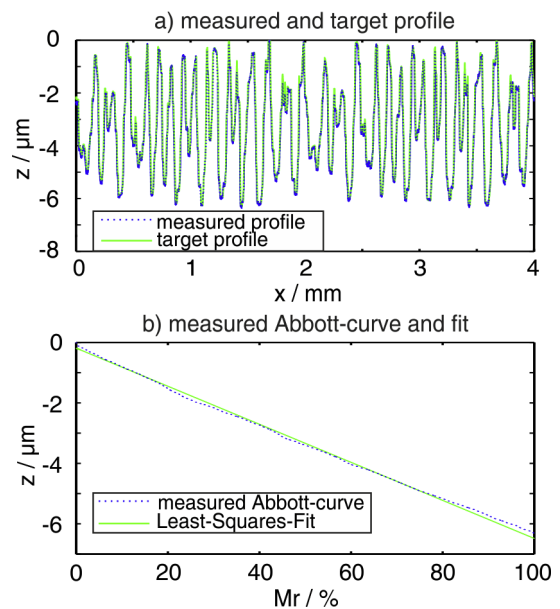|	Stylus instrument	Confocal microscope
$R_a/\mu m$	1.532 ± 0.002	1.501 ± 0.007
$R_q/\mu m$	1.774 ± 0.002	1.742 ± 0.007
$R_z/\mu m$	6.170 ± 0.028	6.142 ± 0.051
$ld/\mu m$	0.059 ± 0.002	0.075 ± 0.007
α_{z2}	0.974 ± 0.001	0.956 ± 0.004
$ld_{ISO2}/\mu m$	0.120 ± 0.005	0.156 ± 0.017
α_{z3}	0.966 ± 0.002	0.943 ± 0.005
$ld_{ISO3}/\mu m$	0.083 ± 0.005	0.104 ± 0.014

Fig. 6. Measurement results (stylus instrument).

results. This means there might be difficulties when applying the designed standard with optical instruments. An extracted profile of the optically measured topography is shown in Fig. 7. The comparison between the measured and the target profile indicates as well a good conformity.

As a parameter study, certain influence factors of the manufacturing process were varied in order to examine their influence on the quality of the standard. The reference standard was manufactured with a constant rotational speed of 800 rpm (cutting speed $v_c = 80.4\ldots160.8$ mm/min), a feed rate of 1 mm/min, a discretization distance of 100 nm and a constant depth of cut of 1 μm. The parameters changed for the parameter study were the discretization distance between two points, the depth of cut and the material used.

The discretization between two points is the resolution of the virtual measurement and hence the resolution of the dataset input for the machine. A resolution of 100 nm corresponds to the resolution of the measurement after manufacturing and was used for the reference standard. To examine the influence of the discretization between two points, the manufacturing resolution was varied to 20 nm.

For the reference, the roughness profile with its global maximum height of the profile of 6.294 μm was manufactured in four cuts. In addition, a standard was manufactured where the whole profile was generated in one cut by varying the depth of cut as defined by the target profile.

The reference standard and the standards with changing discretization distance and varying depth of cut were made of copper. The influence of material was investigated by manufacturing a standard made of brass using the same process parameters as for the reference standard.

The results of the parameter study are summarized in Table 3. For the evaluation, the different roughness parameters and linearity deviations were examined. The mean values and standard deviations of the 1908 evaluation positions for each standard were calculated. The results are as well summarized in Fig. 8.

These results can be used for an adjustment of the z-axis (based on the amplification coefficient α_z as well as for uncertainty estimation of the measurement). In doing so, the amplification coefficient and its standard deviation $\sigma(\alpha_z)$ are required. When a height range h is measured, the maximum systematic deviation u_{sys} can be described based on the amplification coefficient:

$$u_{sys} = h \cdot (1 - \alpha_z). \tag{17}$$

This systematic deviation can be adjusted. However, there is as well a statistical component u_{stat} which can be described based on the standard deviation of the amplification coefficient:

$$u_{stat}(h) = h \cdot \sigma(\alpha_z), \ U_{stat}(h) = k \cdot h \cdot \sigma(\alpha_z), \ k = 2. \tag{18}$$

Because more points are used in comparison to a calibration with step height standards, the uncertainty information gained from this analysis is more reliable.

The following phenomena's can be examined: when the values of the different discretization distances are compared, there is a good conformity of R_a and R_q. Generally it can be shown that the
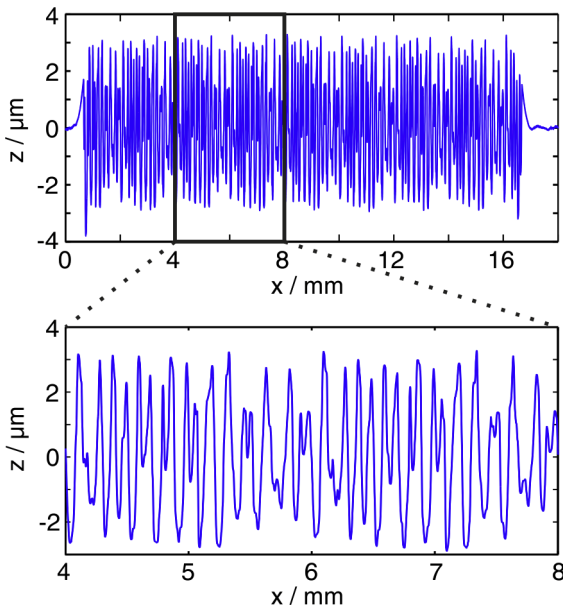

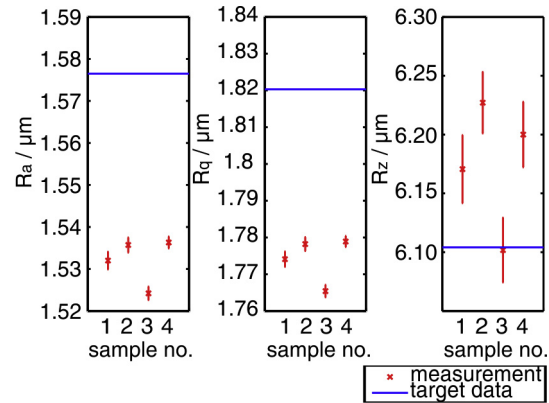Fig. 7. Measurement results (confocal microscope, stitched dataset).

Fig. 8. Results of the performed parameter study, average values and standard deviations given as error-bars.

Table 3
Results of the parameter study.

	Virtual signal	(1) Reference standard	(2) Reduced discretization distance	(3) Varying depth of cut	(4) Different material (brass)
R_a/μm	1.5765	1.532 ± 0.0021	1.536 ± 0.0018	1.524 ± 0.0016	1.536 ± 0.0014
R_q/μm	1.8203	1.774 ± 0.0021	1.778 ± 0.0019	1.765 ± 0.0017	1.779 ± 0.0015
R_z/μm	6.1041	6.170 ± 0.0284	6.227 ± 0.0260	6.101 ± 0.0268	6.200 ± 0.0277
ld/μm	0.0031	0.059 ± 0.0016	0.060 ± 0.0014	0.053 ± 0.0012	0.055 ± 0.0012
α_{z2}	1.0000	0.974 ± 0.0011	0.976 ± 0.0010	0.969 ± 0.0009	0.977 ± 0.0008
ld_{ISO2}/μm	0.0000	0.120 ± 0.0052	0.123 ± 0.0067	0.124 ± 0.0054	0.115 ± 0.0051
α_{z3}	1.0000	0.966 ± 0.0016	0.967 ± 0.0012	0.961 ± 0.0012	0.969 ± 0.0010
ld_{ISO3}/μm	0.0000	0.083 ± 0.0045	0.083 ± 0.0062	0.089 ± 0.0053	0.081 ± 0.0044
ΔR_a/%	–	−2.82	−2.59	−3.32	−2.55
ΔR_q/%	–	−2.54	−2.31	−3.02	−2.27
ΔR_z/%	–	1.09	2.01	−0.05	1.57
			Δ percentage deviation to virtual signal		

manufacturing results are repeatable. The R_z value differs more from the target value as well as the different linearity deviations. One reason why the differences are not really significant is the fact that the later performed sampling has a higher sampling discretization (a measurement resolution of 100 nm) than the virtual discretization of the manufacturing dataset (20 nm). According to theory, there should be no differences as long as the manufacturing resolution is higher than the one of the measurement. This was assured by the machine tool used, providing a resolution of the axes of 20 nm.

When the standard is manufactured with varying depth of cut, the integral roughness parameters deviate a little more from the virtually measured target values, but R_z is very close to its target value. If the manufacturing is executed in one cut, the outer values are achieved with a high fidelity. The slightly smaller standard deviation of the roughness parameters and the fact that the value of *ld* is the lowest within the entire comparison indicates a very good manufacturing and material separation process. This means that the imaged Abbott-curve matches the target Abbott-curve best.

When the different material is examined, it can be observed that the integral roughness parameters are a little closer to the target values and also their standard deviation is slightly smaller. Because the brass has higher hardness values than pure copper, also a better material separation is anticipated as there is less elastic and plastic deformation during the cutting process.

In general, the observed differences between the examined standards are within the nanometer range and therefore within the range of typical values for the stylus instrument measurement uncertainty (see e.g. [30]). This indicates that a repeatable manufacturing process of the roughness standard can be performed. The process is reliable in the examined range of parameters. Summarizing it can be stated that a higher depth of cut and a harder material lead to a slightly reduced standard deviation of the roughness parameters. The best linearity results are achieved when the manufacturing is performed in one cut.

In comparison to the calibration with step height artefacts, the introduced method exhibits an increased effort for the design and manufacturing. This design and manufacturing however needs to be executed only once. The calibration procedure which is performed repeatedly can be executed in a much easier manner as only one measurement is required for the evaluation of the linearity.

5. Conclusion

An algorithm for the model-based generation of a new measurement standard for an almost stepless calibration of the vertical axis linearity was introduced whose "number of steps" is only limited by the spatial discretization of the measured profile. The general feasibility of the manufacturing was shown. Further it was illustrated that the manufactured measurement standard can determine the amplification coefficient and the linearity deviation (both in accordance to ISO 25178-600) as well as a new defined linearity criterion both for tactile and optical measuring devices. However, limitations regarding the application with optical instruments were shown. The influences of different manufacturing parameters were examined. Generally, the manufacturing process is very stable and repeatable. A higher hardness of the material used and an increased depth of cut lead to slightly more stable roughness parameters. For the investigation of the practical use, further investigations are required, e.g. regarding aging effects, the physical interaction with optical measurement devices (the extraction of the electromagnetic surface as defined in ISO 14406 [31]) and the influence of vibrations on the cutting process [32].

Further, design of experiments, as e.g. proposed by Gupt und Kumar [33] could be applied for the parameter optimization.

References

[1] R. Leach, Introduction to surface topography, in: Characterisation of Areal Surface Structure, Springer, Berlin, 2013, pp. 1–14.
[2] J. Frühauf, S. Krönert, Wet etching of silicon gratings with triangular profiles, Microsys. Technol. 11 (12) (2005) 1287–1291.
[3] J. Frühauf, R. Krüger-Sehm, A. Felgner, T. Dziomba, Areal roughness standards, in: Proceedings of the 12th EUSPEN International Conference – Stockholm, 2012, pp. 133–136.
[4] H.H. Gatzen, C. Kourouklis, The fabrication of nano-roughness standards for the calibration of atomic force microscopes, in: Proceedings of the ASPE 16th Annual Meeting, 2001, pp. 493–496.
[5] D. Dornfeld, S. Min, Y. Takeuchi, Recent advances in mechanical micromachining, CIRP Ann. Manuf. Technol. 55 (2) (2006) 745–768.
[6] K. Nemoto, K. Yanagi, M. Aketagawa, I. Yoshida, M. Uchidate, T. Miyaguchi, H. Maruyama, Development of a roughness measurement standard with irregular surface topography for improving 3D surface texture measurement, Meas. Sci. Technol. 20 (2009) 1–7.
[7] U. Brand, T. Kleine-Besten, H. Schwenke, Development of a special CMM for dimensional metrology on microsystem components, in: ASPE 15th Annual Meeting, Scottsdale (Arizona), 2000, pp. 542–546.
[8] H.N. Hansen, R.J. Hocken, G. Tosello, Replication of micro and nano surface geometries, CIRP Ann. Manuf. Technol. 60 (2011) 695–714.
[9] R. Leach, C. Giusca, K. Rickens, O. Riemer, R. Rubert, Development of material measures for performance verifying surface topography measuring instruments, Surf. Topogr.: Metrol. Prop. 2 (2014) 1–5.
[10] ISO 25178-601, Geometrical Product Specifications (GPS) – Surface Texture: Areal – Part 601: Nominal Characteristics of Contact (stylus) Instruments, 2010.
[11] ISO 25178-603, Geometrical Product Specifications (GPS) – Surface Texture: Areal – Part 603: Nominal Characteristics of Non-contact (Phase-shifting Interferometric Microscopy) Instruments, 2013.
[12] J. Seewig, M. Eifler, G. Wiora, Unambiguous evaluation of a chirp measurement standard, Surf. Topogr.: Metrol. Prop. 2 (2014) 045003.
[13] C.L. Giusca, R.K. Leach, F. Helary, T. Gutauskas, L. Nimishakavi, Calibration of the scales of areal surface topography measuring instruments: Part 1. Measurement noise and residual flatness, Meas. Sci. Technol. 23 (2012). 035008.
[14] C. Giusca, R. Leach, F. Helery, Calibration of the scales of areal surface topography measuring instruments: Part 2. Amplification, linearity and squareness, Meas. Sci. Technol. 23 (2012). 065005.
[15] C.L. Giusca, R.K. Leach, Calibration of the scales of areal surface topography measuring instruments: Part 3. Resolution, Meas. Sci. Technol. 24 (2013). 105010.
[16] R.K. Leach, C.L. Giusca, P. Rubert, A single set of material measures for the calibration of areal surface topography measuring instruments: the NPL Areal Bento Box, in: Metrology and Properties of Engineering Surfaces, 2013: Proceedings of the 14th International Conference, Taiwan, 2013, pp. 406–413.
[17] ISO 5436-1, Geometrical Product Specifications (GPS) – Surface Texture: Profile Method Measurement Standards – Part 1: Material Measures, 2000.
[18] ISO 25178-70, Geometrical Product Specification (GPS) Surface Texture: Areal, Part 70: Material Measures, 2014.
[19] Ö. Tan, Effects on the Calibration of Instruments in Surface Metrology: Sensor 2013 Proceedings of the 16th International Conference on Sensors and Measurement Technology – Nürnberg 2013, 297–301.
[20] R. Leach, C. Giusca, Calibration of optical surface topography measuring instruments, in: Optical Measurement of Surface Topography, Springer-Verlag, Berlin Heidelberg, 2011.
[21] Physikalisch-Technische Bundesanstalt: Annual Report 2012, Department 5: Precision Engineering, Braunschweig, 2012, 96–100.
[22] A. Felgner, Normale für die optische Oberflächenmesstechnik, Vortrag, 5. VDI Fachtagung – Metrologie in der Mikro- und Nanotechnik 2013, Nürtingen, 24.10.2013, Germany.
[23] J. Seewig, Eifler M. Neue, praxisorientierte Geometrienormale zur Kalibrierung von Tastschnittgeräten, QZ – Qualität und Zuverlässigkeit 60 (2015), 3, 44–46. Germany.
[24] R. Krüger-Sehm, T. Dziomba, G. Dai, Profile assessment of nano roughness standards by contact and non-contact methods, in: Proc. of the XI. International Colloquium on Surfaces, Part II, 2004, pp. 31–40.
[25] ISO 16610-41, Geometrical Product Specifications (GPS) – Filtration – Part 41: Morphological Profile Filters: Disk and Horizontal Line-segment Filters, 2012.

[26] R. Krüger-Sehm, P. Bakucz, L. Jung, H. Wilhelms, Chirp calibration standards for surface measuring instruments, tm – Tech. Mess. 74 (11) (2007) 572–576.

[27] ISO 16610-21, Geometrical Product Specifications (GPS) – Filtration – Part 21: Linear Profile Filters: Gaussian Filters, 2011.

[28] F. Mauch, W. Lyda, M. Gronle, W. Osten, Improved signal model for confocal sensors accounting for object depending artifacts, Opt. Express 20 (18) (2012) 19936–19945.

[29] H.G. Rhee, W.L. Lee, I.W. Lee, Roughness measurement performance obtained with optical interferometry and stylus method, J. Opt. Soc. Korea 10 (1) (2006) 48–54.

[30] H. Haitjema, Uncertainty analysis of roughness standard calibration using stylus instruments, Precision Eng. 22 (1998) 110–119.

[31] ISO 14406, Geometrical Product Specifications (GPS) – Extraction, 2010.

[32] P.S. Paul, A.S. Varadarajan, R.R. Gnanadurai, Study on the influence of fluid application parameters on tool vibration and cutting performance during turning of hardened steel, Eng. Sci. Technol. Int. J. 19 (2016) 241–253.

[33] M. Gupta, S. Kumar, Investigation of surface roughness and MRR for turning of UD-GFRP using PCA and Taguchi method, Eng. Sci. Technol. Int. J. 18 (2015) 70–81.